Nonlinear electron heating in ultrahigh-intensity-laser–plasma interaction

Erik Lefebvre and Guy Bonnaud
Commissariat à l'Energie Atomique, Centre de Limeil-Valenton, 94195 Villeneuve Saint-Georges, France
(Received 15 May 1996)

The interaction of an ultraintense laser pulse with an overcritical collisionless plasma at normal incidence is investigated with 1.5 dimensional particle-in-cell simulations. Laser absorption and hot electron energy are reported for a large range of intensities and plasma densities. We observe a strong dependence of the electron temperature on the plasma density profile, and a transition between two different heating mechanisms when the gradient length is varied. For sharp edged profiles, the electron temperature is well below the laser ponderomotive potential. [S1063-651X(97)50401-6]

PACS number(s): 52.40.Nk, 52.35.Mw, 52.60.+h

Progress achieved during the last decade in the field of ultrashort and ultraintense lasers makes it now possible to routinely produce, after focusing, intensities I of the order of several 10^{18} W/cm^2, for wavelengths in the range $\lambda_0=0.5$–1 μm and pulse lengths of a few hundred fs full width at half maximum. The transverse momentum gained by an electron in a plane electromagnetic wave is equal to the transverse vector potential of the wave, i.e., in usual units: $p_\perp/m_e c=(I\lambda_0^2/1.4\times10^{18}\ \text{W}\ \mu\text{m}^2/\text{cm}^2)^{1/2}\equiv a_0$. The electron dynamics in such an ultrahigh intensity (UHI) laser wave is then essentially—and not perturbatively—relativistic [1].

At low intensity, an electromagnetic wave of radial frequency ω_0 can propagate up to the so-called critical density $n_c=\omega_0^2 m_e\varepsilon_0/e^2$, where the wave and plasma frequencies become equal. At high intensity, the wave can propagate above n_c [2], so that ''overcritical'' is no longer equivalent to ''opaque.'' In this paper, however, we shall focus on the interaction of a UHI laser pulse with an opaque plasma, at normal incidence. Our results sample the density range 9–$100n_c$, corresponding to $1-12\times10^{22}$ cm^{-3} for 1 μm light. Maximum intensity is around 4×10^{19} W μm^2/cm^2, so that the medium is always opaque to the wave.

An opaque plasma might be heated by resonance absorption [3], vacuum heating [4], $\mathbf{j}\times\mathbf{B}$ heating [5], or different sorts of skin effects [6]. The first two mechanisms are absent in the case of normal incidence in one dimension, since the laser field has no longitudinal component to directly drive the electrons along the density gradient. Yet the magnetic term of the Lorentz force is no longer negligible at high intensity and can play the same role: longitudinal oscillations are excited, which can heat a fraction of the plasma electrons [5]. Two-dimensional (2D) kinetic simulations at moderate densities [7] have shown that a rough approximation for the hot electron temperature was

$$T_h\simeq\phi_p=m_e c^2(\sqrt{1+a_0^2}-1). \tag{1}$$

The physics underlying this formula is straightforward: it equates the characteristic suprathermal energy with the ponderomotive potential of the incident laser wave ϕ_p. Yet the dependence on plasma density is not accounted for in Eq. (1), while intuition as well as 1.5D simulations with denser plasmas [5,8] suggest that it can play an important role. The goal of this paper is thus to elucidate the absorption and suprathermal energy evolution when the parameters $I\lambda_0^2$, n_e/n_c, and the density gradient length L, are varied over a large range of values. We will first address the case of a homogeneous plasma, and then consider the strong influence of the density profile.

The large number of numerical simulations that we wanted to perform precluded the operation of a 2D code. We used the relativistic 1.5D particle-in-cell (PIC) code EUTERPE, in which particle motion under the action of the electromagnetic fields (E_x, E_y, B_z) is described in the three-dimensional phase space x, p_x, p_y. The laser field is thus always linearly polarized, and normally incident on the plasma from the left boundary of the simulation box. We considered finite-length square-shaped pulses of 40 optical cycles (130 fs for 1 μm light). A run is stopped after the tail of the pulse has reflected on the plasma and left the box through the left boundary. Most of the results presented below were obtained with fixed ions, in order to first clarify the electron dynamics. Consequences of ion motion are briefly discussed towards the end of the paper, and a paper on the subject is in preparation. To model the interaction with a massive target, electrons incident on the right boundary of the plasma are absorbed, and reemitted according to their initial thermal distribution. The absorption A can be computed either from the plasma kinetic energy increase, or from the time-integrated Poynting vector fluxes at the system boundaries. Both methods were used, and their excellent agreement is a token of the code accuracy.

Collisions are not included in our simulations, which is a choice consistent with the relatively high value of the initial temperature: $T_{e0}=10$ keV. Then for the highest density that we consider ($n_e=100n_c$) and 1 μm light, $\nu_{ei}/\omega_0\lesssim2\times10^{-3}Z$, justifying a collisionless description. Of course, the plasma will not be created with such a high initial temperature, but the foot of the UHI pulse, interacting with a colder medium, will heat it collisionally up to around 10 keV, where collisionless coupling mechanisms become dominant [9].

The major constraint for this kind of simulation is the need to properly sample the classical skin layer, the width of which is roughly $l_s=c/\omega_p$ [6,8]. We chose for the mesh size $\Delta x\simeq l_s/20$ and used 55 particles per cell in the overcritical plasma. The corresponding time step $\Delta t\sim2\Delta x/c$, can correctly sample the plasma period. When these parameters are

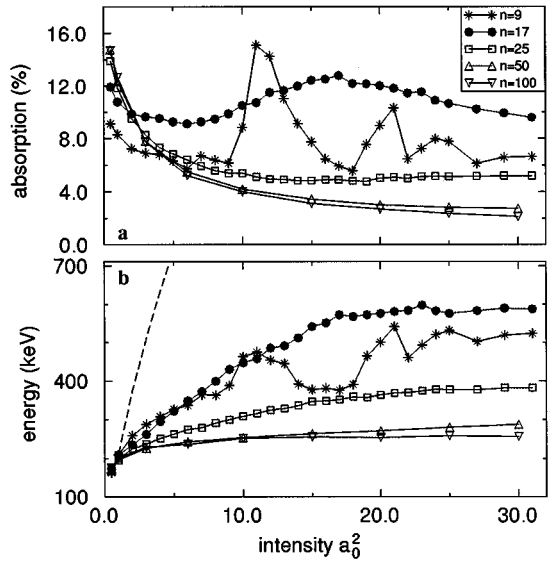

FIG. 1. Absorption (a) and average hot kinetic energy (b) obtained for the interaction of square laser pulse of normalized intensity a_0^2 with a homogeneous plasma of density $n_e=9$, 17, 25, 50, and $100n_c$.

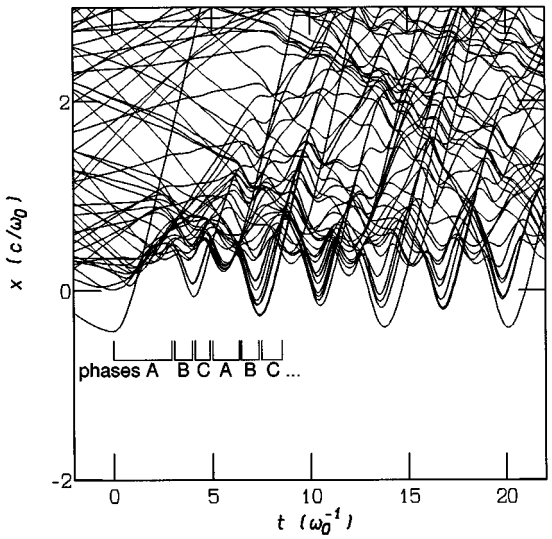

FIG. 2. Trajectories of test electrons in the plasma, for $a_0^2=17$ and $n_e=15n_c$ (the laser wave, incident from below, reaches $x=0$ at $t=0$).

changed by $\pm 20\%$, relative dispersion in the absorption and kinetic energy results $\delta A/A$ and $\delta\langle K_h\rangle/\langle K_h\rangle$ (defined below) is generally less than $\pm 5\%$.

The variations of absorption with intensity are plotted in Fig. 1(a) for five plasma densities. Most of the absorbed energy is carried away through the right edge of the plasma by suprathermal electrons. The suprathermal flux is essentially longitudinal. This could be expected from conservation, at normal incidence, of the transverse generalized momentum of the electrons p_y-eA_y, where A_y is the transverse vector potential. At the right edge of the plasma, where the electromagnetic fields do not propagate, A_y remains nearly equal to its initial value. Hence, the transverse spread of the suprathermal electrons is negligible compared to the longitudinal heating. The distribution function of these particles can generally not be approximated by a Maxwellian distribution, which would be characterized by its temperature T_h. Use of an average energy is more appropriate; to exclude the cold thermal contribution to this average, we compute it for electrons whose energy is higher than 100 keV. Simple calculations with Maxwell–Jüttner functions show that above a temperature of 300 keV; this restricted average is a fairly good approximation of the temperature [10]. The result, denoted $\langle K_h\rangle$, is plotted in Fig. 1(b) for the same parameters as Fig. 1(a). Also plotted on this graph with a dashed line is the ponderomotive potential ϕ_p, independent of plasma density.

At low intensity, as is apparent in Fig. 1(a), absorption grows with plasma density for our range of parameters. This somewhat paradoxical property is, in fact, in good agreement with the results of Ref. [6]: the key parameter $\omega_0^2c^2/\omega_p^2v_{te}^2$ varies from 5.7 for $n_e=9n_c$ to 0.5 for $n_e=100n_c$. For these values, the absorption is mainly due to the so-called sheath inverse bremsstrahlung and is expected to grow with density up to $n_e=50n_c$, which is exactly what we obtain. It is, however, remarkable that those trends predicted in the limit $a_0 \ll v_{te}/c$ are still observed at relativistic intensities.

When the intensity is increased, the variations of absorption indicate that the interaction becomes nonlinear, and even ''turbulent'' for $n_e=9n_c$. Insight can be gained into the heating mechanisms now operating by considering the orbits of test electrons plotted in Fig. 2. The $\mathbf{v}\times\mathbf{B}$ term of Lorentz force has a longitudinal component that acts on the surface electrons; close to the surface, this time-varying contribution is always positive. Around its maximum, it creates a charge separation between the electrons and ions, balanced by a strong electrostatic restoring field (phase A in Fig. 2). When the $\mathbf{v}\times\mathbf{B}$ force decreases, the electrons can expand into vacuum over a distance of the order of $\lambda_0/10$ (phase B). Three effects contribute to dephase their trajectories: the relativistic amplitude of their motion, the variation of plasma frequency with position, and the electromagnetic fields. As a result, particle crossing occurs when the outer electrons reenter the target (phase C) at twice the laser frequency. An effect similar to this ''surface absorption'' had already been identified in the laser wake-field accelerator context, where electrons emitted from the edge of the underdense plasma into vacuum during their oscillations in the plasma wave are injected back into the wave and deplete it [11].

There is no particular reason, in the above scenario, to imply that the hot electron temperature should be equal to the ponderomotive potential. Indeed, in the high-intensity region of Fig. 1(b), the average energy $\langle K_h\rangle$ is considerably lower than ϕ_p, and also less sensitive to the intensity. We expect the plasma density to play a dominant role in the heating process. Let us recall that a free electron, in vacuum $(n_e=0)$, cannot be heated by a plane laser wave [1]. For a finite plasma density, the space charge force will tend to drag back the accelerated electrons until they are deep enough in the target. To gauge the importance of this phenomenon, we have computed the electrostatic potential gap ϕ_s (averaged over two laser cycles during the interaction) between the irradiated and back sides of the target. It turns out to be a very regularly growing function of the intensity, but decreases with plasma density: $e\phi_s/m_ec^2 \sim 0.93a_0^2n_c/n_e$. Assuming that the characteristic electron recoil in the target δx

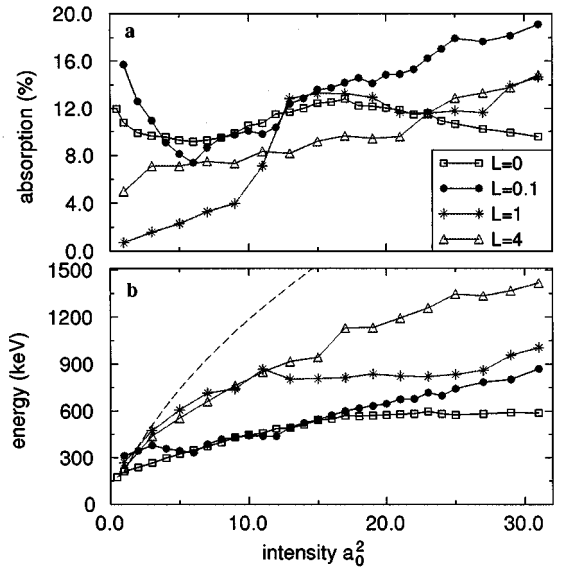

FIG. 3. Absorption (a) and average hot kinetic energy (b) obtained for the interaction of square laser pulse of normalized intensity a_0^2 with an inhomogeneous plasma. Four density profiles are considered: $n_{\max}=17n_c$ with $L=0$, 0.1, and 1, and $n_{\max}=9n_c$ with $L=4c/\omega_0$.

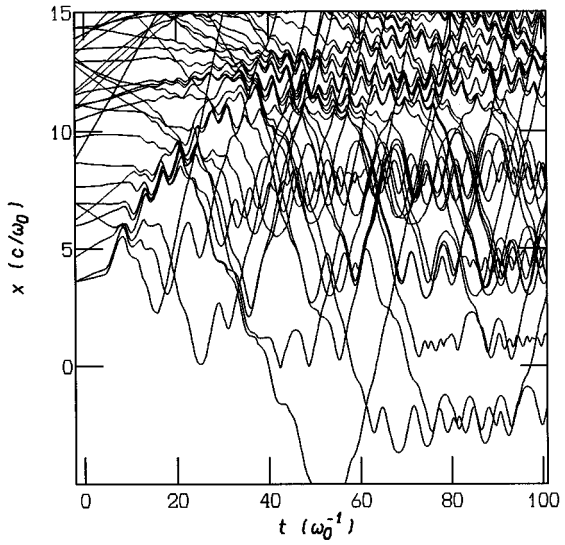

FIG. 4. Trajectories of test electrons around the edge of the plasma, for $a_0^2=17$, $n_{\max}=9n_c$, and $L=3c/\omega_0$.

is given by a balance between the electrostatic and $\mathbf{v}\times\mathbf{B}$ forces, we obtain $n_e\delta x=a_0v_y/c\sim a_0$, which yields the same scaling $\phi_s\propto n_e\delta x^2=a_0^2n_c/n_e$. At low intensity, ϕ_s is smaller than $\langle K_h\rangle$, but it always eventually overshoots $\langle K_h\rangle$, at a value of a_0^2 that increases with density. This strong space charge illustrates both the slowing down of suprathermals by density effects, and the efficiency of electron heating at high intensity and low density. (In mobile ion simulations, ϕ_s would also drag the ions into the target and steepen the density profile.)

The results presented above were obtained for a homogeneous plasma with a sharp boundary. Yet, a finite, even small, gradient length can have a drastic influence on the interaction. The density profiles that we now consider are of the type $n_e(x)=xn_c/L$ from $x=0$ to $x=Ln_{\max}/n_c$, followed by a plateau at density $n_{\max}$. A homogeneous plasma corresponds to the limiting case $L=0$.

As we did in Fig. 1 for $L=0$, we represent in Fig. 3, as a function of intensity, the absorption and average energy of suprathermal electrons for different gradient lengths. Results for $n_e=17n_c$, $L=0$ are also plotted for completeness. For a small gradient length ($L=0.1c/\omega_0$), the differences with the homogeneous case are most pronounced at high intensity: the absorption is larger (up to a factor of 2), and the electrons are slightly hotter. For a smoother profile, the most striking change lies in the increased average energy. On the whole, the average energy increases with gradient length, and a more regular growth of absorption with intensity is observed in an inhomogeneous profile.

The nonlinear heating mechanism that we previously pointed at must be revised for an inhomogeneous plasma. The incident and reflected waves form a nearly standing pattern in front of the target. When the density gradient is smooth enough, the laser reflection point is located inside the plasma, and the electrons that are below this turning point interact with this standing wave. It makes them oscillate stochastically with a large longitudinal amplitude, as was recently studied in a more academic way by Bauer *et al.* [12]. It is apparent in Fig. 4 that during these oscillations, some particles can randomly escape the interaction region and run into the target. On the other hand, hot electron generation at the laser turning point is now reduced: a sharp density jump at the reflection point is crucial in dephasing the electron trajectories, a condition that is only fulfilled for a small gradient length. This heating process, which we term ''volume absorption,'' is very similar to that observed during the phenomenon of self-induced transparency [2]: the same longitudinal oscillations can be observed behind the transparency front, where the incident and reflected waves also form a large amplitude standing wave.

Finally, we can hold the laser intensity and maximum plasma density fixed, but change the gradient length. The absorption and energy variations in this case are plotted in Fig. 5 for $n_{\max}=9n_c$ and three different intensities. As previously noticed, the average energy grows with intensity and gradient length. Absorption reaches a first maximum for a small value of L, decreases and then grows again. The first maxima, observed at small gradient lengths, are, in fact, similar to the strong variations in absorption observed for a homogeneous plasma at ''low'' density ($n_e=9n_c$ in Fig. 1). Absorption in this regime is very sensitive to the details of plasma surface. A tiny layer of electrons in front of the reflection point will not drastically affect field propagation, but will be very efficiently driven by the $\mathbf{v}\times\mathbf{B}$ force and accelerated out of phase with the bulk of surface electrons. Average energy and absorption are then increased, since the slowing by the ambipolar field is lower for these specific electrons. When the gradient length is further increased, electron trajectories at the reflection point are no longer out of phase and less hot particles are generated there. On the other hand, there is now enough underdense plasma for volume heating to develop, and absorption eventually grows again with gradient length, due to this second mechanism. For still smoother gradient length (up to $L=14\sim2.2\lambda_0$), absorption keeps increasing with L, up to values of the order of ϕ_p (see Fig. 5).

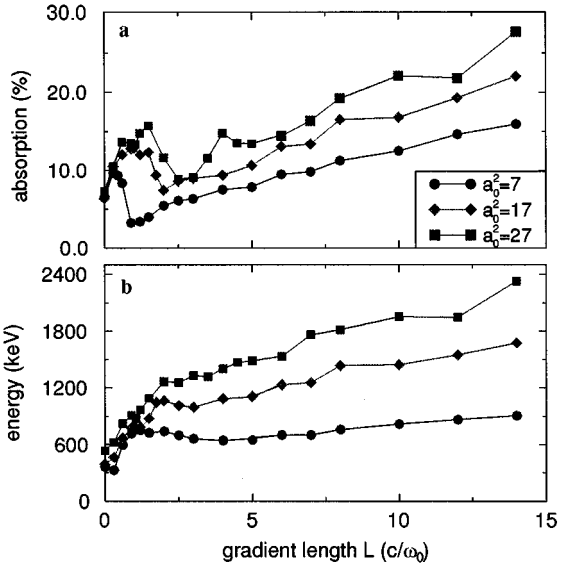

FIG. 5. Absorption (a) and average hot kinetic energy (b) obtained for the interaction of square laser pulse with a plasma of maximum density $n_{\max}=9n_c$ and variable density gradient L, for three different intensities $a_0^2=7$, 17, and 27. The corresponding ponderomotive potentials are $\phi_p=930$, 1660, and 2190 keV, respectively.

We eventually performed some simulations with mobile ions ($m_i/Zm_e=3672$), in order to check our major assumption of a fixed ion background. The electron energy is always reduced in this case, since due to profile steepening, heating now occurs in a region of higher density. For sharp edged plasmas, absorption is slightly increased (say, by one third), but this increase is much more important (roughly a factor of 2) for a smooth initial density profile. Note that these increases essentially result from a better absorption in electrons, not in ions. In spite of profile modification, it is still relevant to make a distinction between the two heating mechanisms observed for fixed ions. Ponderomotive steepening only occurs around the laser reflection point: the low-density foot of a smooth profile will not be swept off, and volume absorption can take place there. But in addition, a sharp density jump can develop at the laser reflection point, favorable to surface absorption. Hence, both coupling mechanisms can take place simultaneously in a smooth edged plasma when mobile ions are considered, leading to a higher overall absorption.

In conclusion, our simulations spanning a large range of interaction conditions revealed three distinct coupling mechanisms. Skin effect predictions appear to be relevant up to a moderate intensity ($a_0^2\lesssim 1$). At higher intensity, the nonlinear coupling drastically depends on the initial density profile: for sharp profiles, the hot electron average energy is definitely below the ponderomotive potential, and the absorption is low ($\lesssim 10\%$). When the density gradient is flattened, a transition from surface to volume absorption is observed, the latter generating hotter suprathermal distributions and leading to a higher coupling efficiency (30% at maximum). The inclusion of ion motion in our simulations slightly lowers the hot electron temperature, but the absorption increase can be important. Our results emphasize the need of an accurate knowledge of the initial plasma conditions to quantitatively interpret UHI laser-plasma experiments; they also suggest that recent experiments under similar conditions [13] were affected by the expansion of a preplasma in front of the target, at the very beginning of the interaction.

The authors acknowledge interesting discussions on related topics with A. Andreev, A. Bers, J. Denavit, T. W. Johnston, G. Malka, P. Rambo, J.-M. Rax, and S. C. Wilks.

[1] E. S. Sarachik and G. T. Schappert, Phys. Rev. D **1**, 2738 (1970).
[2] E. Lefebvre and G. Bonnaud, Phys. Rev. Lett. **74**, 2002 (1995).
[3] K. Estabrook and W. L. Kruer, Phys. Rev. Lett. **40**, 42 (1978).
[4] F. Brunel, Phys. Rev. Lett. **59**, 52 (1987); G. Bonnaud, P. Gibbon, J. Kindel, and E. Williams, Laser Part. Beams **9**, 339 (1991); P. Gibbon and A. R. Bell, Phys. Rev. Lett. **68**, 1535 (1992).
[5] W. L. Kruer and K. Estabrook, Phys. Fluids **28**, 430 (1985).
[6] T.-Y. Brian Yang, W. L. Kruer, R. M. More, and A. B. Langdon, Phys. Plasmas **2**, 3146 (1995).
[7] S. C. Wilks, W. L. Kruer, M. Tabak, and A. B. Langdon, Phys. Rev. Lett. **69**, 1383 (1992); S. C. Wilks, Phys. Fluids B **5**, 2603 (1993).
[8] J. Denavit, Phys. Rev. Lett. **69**, 3052 (1992).
[9] J. Delettrez, Laboratory for Laser Energetics Quarterly Report **58**, 76 (1994); P. Rambo (private communication).
[10] Note that for a relativistic distribution, the temperature is no longer equal to twice the average kinetic energy.
[11] G. Bonnaud, D. Teychenné, and J.-L. Bobin Europhys. Lett. **26**, 91 (1994).
[12] J.-M. Rax, Phys. Fluids B **4**, 3962 (1992); D. Bauer, P. Mulser, and W.-H. Steeb, Phys. Rev. Lett. **75**, 4622 (1995).
[13] G. Malka and J.-L. Miquel, Phys. Rev. Lett. **77**, 75 (1996).